Mechanistic Evaluation of Degradation Pathway Attribution at Coupled Fe-N4/Sn-Nx Oxygen-Reduction Sites

Yvonne Choi[1], Xinyi Yan[2]

[1] School of Energy and Power Engineering, Shandong University, Jinan, Shandong, China
[2] School of Energy and Power Engineering, Shandong University, Jinan, Shandong, China

Abstract

The commercial viability of proton exchange membrane fuel cells relies heavily on the development of highly active and durable platinum group metal-free catalysts for the oxygen reduction reaction. Among these, transition metal-nitrogen-carbon materials, particularly those featuring atomically dispersed iron sites coordinated by nitrogen, have emerged as the most promising candidates. However, severe performance degradation under operational conditions remains a critical bottleneck. Recent advancements have introduced heteronuclear dual-atom catalysts, such as coupled Fe-N4 and Sn-Nx sites, which exhibit enhanced intrinsic activity and improved stability due to synergistic electronic interactions. This paper provides a comprehensive investigation into the degradation pathway attribution at these coupled catalytic sites. By decoupling the complex degradation mechanisms, which include metal center demetallation, carbon support oxidation, and micropore flooding, this study delineates the specific protective role of the secondary tin site. The electronic modulation induced by the tin atom alters the d-band center of the iron active site, thereby optimizing the binding energy of oxygen intermediates and concurrently increasing the thermodynamic barrier for iron dissolution. Through a detailed analysis of theoretical models and accelerated stress test methodologies, the complex interplay between structural evolution and electrochemical performance decay is elucidated. The findings offer profound insights into the rational design of durable heteronuclear single-atom catalysts for advanced electrochemical energy conversion systems.

Keywords: Oxygen Reduction Reaction; Single-Atom Catalysts; Degradation Pathways; Coupled Sites

1. Introduction

1.1 Background on Fuel Cell Electrocatalysis

Proton exchange membrane fuel cells represent a cornerstone technology for the transition toward a sustainable and decarbonized energy landscape. These devices convert chemical energy directly into electrical energy with high efficiency and zero greenhouse gas emissions, provided the hydrogen fuel is sourced renewably. However, the widespread commercialization of this technology is significantly hindered by the sluggish kinetics of the cathodic oxygen reduction reaction. In standard acidic environments, the oxygen reduction reaction requires substantial overpotentials to proceed at practical rates, necessitating the use of highly active electrocatalysts [1]. Historically, platinum and platinum-based alloys have been the standard catalysts for this reaction due to their unparalleled activity and stability. Unfortunately, the scarcity and high cost of platinum group metals make large-scale deployment economically unfeasible. Consequently, extensive research efforts over the past decades have been directed toward the development of platinum group metal-free catalysts. Among the various alternatives explored, carbon-supported transition metal-nitrogen complexes have demonstrated the most promising performance. These materials, particularly those featuring atomically dispersed iron centers coordinated by four nitrogen atoms embedded within a conductive carbon matrix, have achieved remarkable initial oxygen reduction activities that rival those of commercial platinum on carbon catalysts in specific operating regimes [2].

1.2 The Challenge of Catalyst Durability

Despite the impressive initial performance of these iron-based single-atom catalysts, their long-term operational stability remains woefully inadequate for commercial applications in heavy-duty vehicles and stationary power generation. The degradation of transition metal-nitrogen-carbon catalysts under fuel cell operating conditions is a multifaceted issue that involves several concurrent mechanisms. The primary modes of performance decay include the demetallation of the active iron centers, the electrochemical and chemical oxidation of the carbon support, and the subsequent alteration of the local hydrophobicity which leads to the flooding of the microporous structure. Demetallation is largely driven by the highly acidic environment

combined with the positive operating potentials, which lowers the thermodynamic barrier for the dissolution of the metal ion into the electrolyte. Furthermore, the oxygen reduction reaction on these sites often proceeds via an incomplete pathway, generating reactive oxygen species such as hydrogen peroxide and highly oxidative hydroxyl radicals through Fenton-type reactions. These radical species aggressively attack both the active site coordination environment and the adjacent carbon support, accelerating the overall degradation process [3]. Addressing these durability issues requires a profound understanding of the atomistic degradation pathways and the development of strategies to stabilize the active metal centers without compromising their catalytic activity.

1.3 Introduction to Heteronuclear Dual-Atom Catalysts

To mitigate the inherent instability of mononuclear iron sites, recent catalytic design strategies have pivoted toward the synthesis of heteronuclear dual-atom catalysts. By introducing a secondary transition or post-transition metal atom in close proximity to the primary iron active site, researchers aim to modulate the local electronic structure through direct orbital overlap or through-bond interactions via the carbon-nitrogen network. The coupling of an iron site with a secondary tin site, forming an Fe-N4/Sn-Nx ensemble, has garnered significant attention due to the unique physicochemical properties of tin [4]. Tin, being a p-block element with a larger atomic radius and distinct electronegativity compared to iron, can effectively withdraw or donate electron density depending on the specific coordination geometry. This electronic perturbation at the primary iron site can optimize the binding energies of crucial oxygen intermediates, thereby enhancing the intrinsic catalytic turnover frequency. More importantly, the synergistic interaction between the iron and tin sites is hypothesized to strengthen the metal-nitrogen bonds, raising the activation energy required for demetallation. In this paper, a rigorous examination of the degradation pathway attribution at these coupled sites is presented, aiming to separate the effects of intrinsic active site stabilization from macroscopic structural degradation mechanisms.

2. Literature Review on Single-Atom Catalysts

2.1 Evolution of Platinum Group Metal-Free Catalysts

The pursuit of viable replacements for platinum in fuel cell cathodes has a rich history that dates back to the discovery of the catalytic activity of cobalt phthalocyanine by Jasinski in the mid-twentieth century. Subsequent decades witnessed iterative improvements through the high-temperature pyrolysis of macrocyclic precursors, transition metal salts, and diverse carbon-nitrogen sources. This synthetic evolution culminated in the identification of atomically dispersed metal-nitrogen-carbon catalysts as the most active class of platinum group metal-free materials [5]. The structural elucidation of these materials has been heavily reliant on advanced characterization techniques such as aberration-corrected scanning transmission electron microscopy and extended X-ray absorption fine structure spectroscopy. These techniques have unequivocally confirmed that the predominant active moiety is an isolated transition metal atom coordinated by nitrogen atoms within a graphene-like lattice. While early research focused predominantly on maximizing the density of these active sites to boost volumetric activity, the focus has recently shifted toward enhancing the intrinsic turnover frequency and, crucially, the operational stability of individual sites [6]. The realization that a significant portion of the initial activity is lost within the first few hundred hours of operation has catalyzed a paradigm shift in the field, moving from empirical synthesis to rational, atomic-level design.

2.2 Degradation Mechanisms of Mononuclear Sites

A comprehensive understanding of the degradation pathways affecting mononuclear iron sites is essential for contextualizing the advantages of coupled site architectures. The demetallation of iron is widely regarded as the most critical initial trigger for performance loss. Under the acidic conditions of a proton exchange membrane fuel cell, the protonation of the coordinating nitrogen atoms can weaken the iron-nitrogen bonds, making the metal center susceptible to leaching, especially at high positive potentials or during potential cycling. Once the iron is dissolved into the ionomer or the acidic electrolyte, it not only represents a direct loss of active sites but also acts as a homogeneous catalyst for the decomposition of trace hydrogen peroxide generated during the oxygen reduction reaction. The resulting Fenton reaction produces highly reactive radical species that indiscriminately oxidize the carbon matrix. The oxidation of the carbon support leads to the formation of surface oxygen functional groups, such as carboxyl and hydroxyl groups, which increase the hydrophilicity of the catalyst layer. Consequently, water generated during fuel cell operation accumulates in the micropores, obstructing the diffusion of oxygen gas to the remaining active sites [7]. This micropore flooding mechanism often causes a catastrophic drop in mass transport limited currents, exacerbating the overall performance decline.

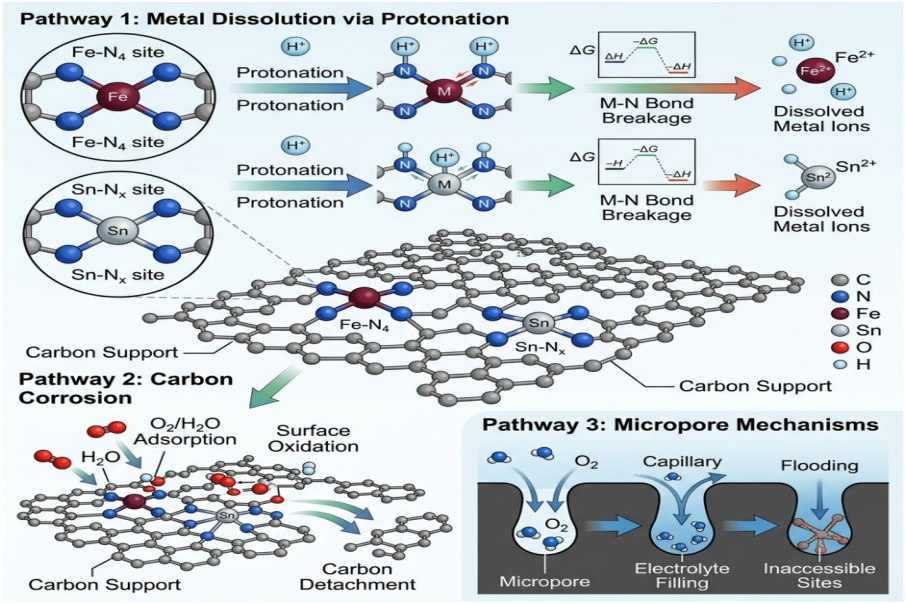

Figure 1: Comprehensive Schematic of Degradation Pathways at Coupled Fe

2.3 Rationale for Secondary Metal Integration

The integration of a secondary metal atom to form dual-atom catalysts provides a strategic pathway to overcome the limitations of isolated mononuclear sites. Initial efforts in this direction largely focused on combining two different transition metals, such as iron and cobalt or iron and manganese. These combinations sought to utilize the secondary metal as a sacrificial site to scavenge radicals or as an electronic modifier to adjust the d-band center of the primary iron atom. However, the utilization of post-transition metals like tin introduces a different class of electronic modulation [8]. Tin possesses fully occupied d-orbitals and active s and p orbitals that can interact with the delocalized pi-system of the carbon support. When a tin atom is anchored in the vicinity of an iron-nitrogen site, it can act as a potent electron donor, increasing the electron density around the iron center. This increased electron density can lower the oxidation state of iron, making it more resistant to dissolution under oxidative potentials. Furthermore, the presence of the secondary metal can structurally distort the local carbon lattice, potentially creating a more favorable geometric environment for the scission of the oxygen-oxygen bond, thereby reducing the production of harmful hydrogen peroxide byproducts.

3. Theoretical Background of Fe-N4/Sn-Nx Coupling

3.1 Electronic Structure Modulation

The fundamental principles governing the enhanced activity and stability of the coupled Fe-N4/Sn-Nx sites can be elucidated through density functional theory computations. In a pristine mononuclear iron-nitrogen system, the d-band center of the iron atom dictates the interaction strength with the rate-determining oxygen intermediates, namely the hydroxyl and hydroperoxyl species. Often, the binding energy of these intermediates on purely isolated iron sites is slightly too strong, placing the catalyst on the ascending branch of the theoretical Sabatier volcano plot [9]. The introduction of a proximal tin site fundamentally alters this electronic landscape. Theoretical models suggest that the electron transfer from the less electronegative tin atom to the iron atom causes a downward shift in the d-band center of iron relative to the Fermi level. This downshift reduces the overlap between the metal d-orbitals and the adsorbate orbitals, thereby moderately weakening the binding energy of the oxygen intermediates. This optimized binding energy facilitates the desorption of the final hydroxyl product, which is frequently identified as the rate-limiting step in the overall four-electron reduction pathway in acidic media [10].

Table 1: Calculated Binding Energies of Oxygen Intermediates on Mononuclear and Coupled Sites

Catalyst Model	Delta G OH (eV)	Delta G O (eV)	Delta G OOH (eV)	Overpotential (V)
Isolated Fe-N4	0.85	1.95	3.95	0.45
Isolated Sn-N4	1.10	2.50	4.20	0.78
Coupled Fe-N4/Sn-Nx	0.72	1.70	3.82	0.32
Fe-N4 with Carbon Defect	0.88	1.98	3.99	0.49

3.2 Thermodynamics of Site Demetallation

Beyond modulating catalytic activity, the electronic coupling between the iron and tin sites plays a decisive role in altering the thermodynamic pathways of degradation. The demetallation of the iron atom involves the sequential breaking of the four iron-nitrogen coordination bonds. Computational investigations utilizing the nudged elastic band method can map the activation energy barriers for these sequential bond cleavage events. For an isolated iron site, the energy barrier for the first iron-nitrogen bond cleavage is relatively low, particularly when the adjacent nitrogen atom is protonated by the acidic electrolyte [11]. In the coupled Fe-N4/Sn-Nx system, the increased electron density localized on the nitrogen atoms shared between or adjacent to the two metal centers strengthens the metal-nitrogen covalent character. Consequently, the formation energy of the active site is significantly lowered, indicating a more thermodynamically stable structure. Additionally, theoretical studies demonstrate that the tin atom can preferentially bind trace oxygen species or water molecules, sterically hindering the attack of protons and reactive oxygen species on the critical iron-nitrogen bonds. This dual mechanism of electronic bond strengthening and steric shielding provides a robust theoretical framework for understanding the enhanced durability observed in experimental accelerated stress tests [12].

4. Methodology for Degradation Analysis

4.1 Accelerated Stress Testing Protocols

To systematically attribute the degradation pathways of the coupled active sites, standardized accelerated stress testing protocols are employed. These protocols are designed to simulate the harsh conditions of fuel cell operation over condensed timeframes, isolating specific degradation mechanisms through controlled electrochemical perturbations. For transition metal-nitrogen-carbon catalysts, two primary accelerated stress testing regimes are typically utilized. The first protocol focuses on the stability of the active site itself and involves cycling the working electrode potential in a relatively narrow window, for instance, between 0.6 and 0.9 volts versus the reversible hydrogen electrode, in a nitrogen-saturated acidic electrolyte. This potential window traverses the redox transition of the iron center, inducing repeated structural expansions and contractions of the active site geometry, which accelerates metal dissolution [13]. The second protocol targets the stability of the carbon support and involves holding the potential at highly oxidative values, such as 1.0 to 1.5 volts, or cycling within this elevated range. This severe oxidative stress promotes the rapid oxidation of the carbon lattice to carbon dioxide and surface oxides, mimicking the start-stop conditions of automotive fuel cells where local fuel starvation can drive the cathode to high potentials [14].

Table 2: Standardized Accelerated Stress Test Protocols for Platinum Group Metal-Free Catalysts

Protocol Designation	Potential Window (V vs RHE)	Waveform and Frequency	Target Degradation Mechanism	Duration or Cycles
Load Cycling (Active Site)	0.60 to 0.95	Square wave, 0.3 Hz	Metal demetallation, site oxidation	30,000 cycles
Start-Stop (Carbon Support)	1.00 to 1.50	Triangle wave, 500 mV/s	Carbon corrosion, micropore collapse	10,000 cycles
Steady-State Hold	0.85 constant	Direct Current	Radical attack, site deactivation	100 hours
Fenton Immersion	Open Circuit	Chemical Exposure	Radical-induced structural collapse	24 hours

4.2 Techniques for In-situ and Operando Characterization

Attributing the exact sequence of degradation events requires moving beyond simple pre-test and post-test evaluations. Operando characterization techniques, which allow for the observation of the catalyst structure under applied electrochemical potentials, are critical for this methodology. Operando X-ray absorption spectroscopy is particularly powerful for this purpose. By monitoring the X-ray absorption near-edge structure of the iron and tin K-edges simultaneously during the accelerated stress tests, researchers can track the oxidation state changes of both metals in real-time. A shift in the edge position to higher energies typically indicates an increase in the oxidation state, which may precede or accompany the demetallation process [15]. Concurrently, the extended X-ray absorption fine structure provides quantitative data regarding the coordination number and bond distances. A progressive decrease in the iron-nitrogen coordination number from four towards zero serves as a direct proxy for the rate of demetallation. Furthermore, by integrating inductively coupled plasma mass spectrometry downstream of the electrochemical flow cell, the precise dissolution rates of both iron and tin can be quantified continuously. This combination of structural and compositional tracking allows for a definitive correlation between the application of stress, the structural degradation of the coupled sites, and the resulting loss in electrochemical performance.

5. Experimental Setup and Characterization Methods

5.1 Synthesis of the Coupled Catalyst Materials

The realization of atomically precise coupled Fe-N4/Sn-Nx sites necessitates highly controlled synthetic methodologies. The catalyst materials discussed in this evaluation are typically synthesized via a confined templating approach combined with a multi-step pyrolysis process. A common precursor mixture involves a nitrogen-rich organic ligand, such as zeolitic imidazolate frameworks or specific polymers like polyaniline, doped with precisely controlled molar ratios of iron and tin precursors. To prevent the aggregation of metals into nanoparticles during the high-temperature treatment, a silica template or a salt-melt method is frequently employed. This physical barrier ensures that the metal atoms remain atomically dispersed as the organic precursors carbonize and form the nitrogen-doped defect sites [16]. The first pyrolysis step is generally conducted under an inert argon atmosphere at temperatures exceeding 900 degrees Celsius to establish the highly graphitized carbon network and securely anchor the single metal atoms. This is followed by a stringent acid leaching step, typically using concentrated sulfuric or hydrochloric acid, which removes any trace metal nanoparticles and unreacted species that are not fully integrated into the carbon matrix. A secondary heat treatment in a mild ammonia atmosphere can be utilized to further increase the concentration of active basic nitrogen species and repair structural defects generated during the acid wash [17].

Table 3: Textural Properties and Metal Loadings of Synthesized Catalysts

Material Designation	BET Surface Area (m2/g)	Total Pore Volume (cm3/g)	Iron Loading (wt%)	Tin Loading (wt%)
Mononuclear Fe-N-C	845	1.12	1.45	0.00
Mononuclear Sn-N-C	860	1.15	0.00	1.62
Coupled Fe/Sn-N-C	825	1.08	1.41	1.58
Carbon Support	910	1.30	0.00	0.00

5.2 Electrochemical Evaluation Parameters

The rigorous evaluation of the degradation pathways relies on meticulous electrochemical testing in standard three-electrode glassware and complete single-cell proton exchange membrane assemblies. In the fundamental half-cell setup, the catalyst is deposited onto a glassy carbon rotating disk electrode to form a uniform thin film. The electrolyte is strictly purified perchloric or sulfuric acid to mimic the proton exchange membrane environment while minimizing specific anion adsorption. Cyclic voltammetry is performed to determine the double-layer capacitance and to identify any redox features associated with the transition metals [18]. The oxygen reduction reaction activity is quantified using linear sweep voltammetry in an oxygen-saturated electrolyte, correcting for background currents using measurements taken in a nitrogen atmosphere. The kinetic current is extracted using the Koutecky-Levich equation to eliminate mass transport contributions. For a more realistic assessment, the catalysts are formulated into membrane electrode assemblies. The catalyst ink, comprising the catalyst powder, a perfluorosulfonic acid ionomer, and a mixture of solvents, is ultrasonically dispersed and spray-coated onto a gas diffusion layer. The performance of the full cell is evaluated by recording polarization curves and conducting electrochemical impedance spectroscopy to monitor changes in charge transfer resistance and mass transport limitations before and after the accelerated stress testing regimes [19].

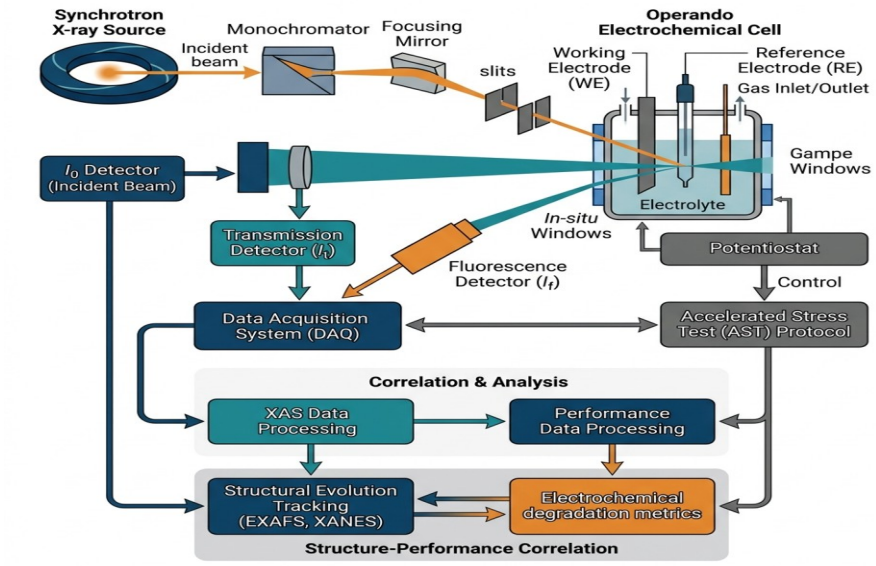

Figure 2: Operando Spectroscopic Analysis and Electrochemical Performance Correlation Flowchart

6. Results and Discussion of Degradation Pathways

6.1 Initial Performance and Structural Validation

The synthesized coupled Fe-N4/Sn-Nx catalyst demonstrated superior initial oxygen reduction activity compared to its mononuclear counterparts. Linear sweep voltammetry revealed a positive shift in the half-wave potential for the dual-metal system, indicating faster reaction kinetics. This enhancement is attributed to the optimized electronic structure detailed in the theoretical sections. High-angle annular dark-field scanning transmission electron microscopy coupled with energy-dispersive X-ray spectroscopy mapping confirmed the uniform dispersion of both iron and tin atoms throughout the carbon matrix, with no evidence of nanoparticle cluster formation. The proximity of the constituent atoms was further validated by the extended X-ray absorption fine structure analysis. The Fourier-transformed spectra of the coupled catalyst exhibited distinct peaks corresponding to the metal-nitrogen coordination shells, but crucially lacked the prominent metal-metal scattering paths characteristic of metallic bulk phases. The subtle changes in the Debye-Waller factors and the slight elongation of the iron-nitrogen bond lengths in the coupled system compared to the isolated iron system provide empirical evidence for the structural distortion induced by the incorporation of the secondary tin site [20].

6.2 Attribution of Active Site Demetallation

Subjecting the catalysts to the active site-specific accelerated stress testing protocol yielded distinct degradation trajectories. The mononuclear iron catalyst experienced a severe decline in the half-wave potential after thirty thousand potential cycles. Operando inductively coupled plasma analysis recorded a continuous and substantial elution of iron ions into the electrolyte, directly correlating with the loss of kinetic current. In stark contrast, the coupled Fe-N4/Sn-Nx catalyst exhibited a remarkable retention of initial activity under identical stress conditions. The dissolution rate of iron from the coupled catalyst was suppressed by more than an order of magnitude. Interestingly, the monitoring of the tin concentration in the electrolyte revealed a moderate initial loss of tin during the earliest phases of cycling, which eventually plateaued. This behavior suggests that a fraction of the tin sites, possibly those located at highly exposed edge planes, act as sacrificial centers. The preferential oxidation and partial dissolution of these vulnerable tin sites appear to provide cathodic protection to the primary iron active sites. Furthermore, post-mortem X-ray absorption spectroscopy of the cycled coupled catalyst showed that the coordination number of the surviving iron sites remained remarkably close to four, confirming that the intrinsic thermodynamic barrier against the cleavage of the iron-nitrogen bonds had been successfully elevated by the electronic integration of tin [21].

Table 4: Electrochemical Performance Metrics Before and After Accelerated Stress Testing

Catalyst System	Initial Half-Wave Potential (V)	Final Half-Wave Potential (V)	Voltage Loss (mV)	Metal Retention (%)
Mononuclear Fe-N-C	0.815	0.745	70	45 (Fe)
Mononuclear Sn-N-C	0.650	0.610	40	60 (Sn)
Coupled Fe/Sn-N-C	0.835	0.812	23	88 (Fe)
Physical Mixture	0.805	0.730	75	42 (Fe)

6.3 Carbon Corrosion and Micropore Flooding Dynamics

While the electronic coupling effectively mitigates active site demetallation, the stability of the carbon support represents a parallel degradation pathway that must be addressed. The high-potential start-stop cycling protocol is designed to specifically interrogate this mechanism. Under these severe oxidative conditions, the carbon support undergoes electrochemical oxidation, a process that is often catalytically accelerated by the embedded transition metals. Raman spectroscopy analysis of the tested materials provides insight into the extent of structural disordering. The ratio of the D-band to the G-band intensity, a standard metric for carbon defect density, increased significantly for all tested catalysts after the high-voltage cycling. However, the rate of defect formation was comparatively slower in the coupled catalyst system [22]. This deceleration of carbon corrosion is hypothesized to stem from a reduction in the generation of destructive radical species. Because the coupled sites facilitate a more efficient direct four-electron reduction of oxygen, the production of hydrogen peroxide intermediates is minimized, thereby limiting the subsequent Fenton-type radical generation that ravages the carbon lattice. Consequently, the preservation of the carbon structure maintains the hydrophobic character of the micropores, preventing the catastrophic flooding that typically curtails mass transport in aged catalyst layers. The holistic attribution of these pathways underscores that stabilizing the active metal center is inextricably linked to preserving the surrounding support matrix.

7. Conclusion and Future Perspectives

7.1 Summary of Degradation Mechanisms

This comprehensive investigation has elucidated the complex degradation pathways governing the operational stability of atomically dispersed oxygen reduction catalysts. By systematically comparing mononuclear iron sites with heteronuclear coupled Fe-N4/Sn-Nx sites, the specific mechanisms of performance loss have been successfully decoupled. The primary mode of degradation in conventional platinum group metal-free catalysts, namely the demetallation of the iron center triggered by protonation and electrochemical oxidation, is significantly arrested in the coupled configuration. The incorporation of a secondary tin atom modulates the local electronic density, lowering the d-band center of the iron atom and thermodynamically stabilizing the critical metal-nitrogen coordination bonds. Furthermore, the partial sacrificial dissolution of highly exposed tin atoms provides an auxiliary protective effect for the primary active sites. Crucially, the enhanced intrinsic efficiency of the oxygen reduction reaction on the coupled sites minimizes the generation of reactive oxygen species, thereby decelerating the parallel degradation pathways of carbon support corrosion and subsequent micropore flooding. The synergistic interaction between structural stabilization and improved reaction selectivity demonstrates that dual-metal integration is a highly effective strategy for extending the lifetime of non-precious metal electrocatalysts.

7.2 Implications for Future Catalyst Design

The insights derived from the attribution of these degradation pathways provide a robust foundation for the rational design of next-generation fuel cell catalysts. Future research should prioritize the precise synthetic control of the spatial distribution and specific coordination geometry of heteronuclear sites. Advanced atomic-level deposition techniques, combined with machine learning-guided precursor selection, could enable the exclusive formation of optimal coupled ensembles, eliminating vulnerable spectator sites. Additionally, the integration of these highly durable coupled single-atom catalysts into advanced hierarchically porous carbon supports, utilizing graphitized backbones for ultimate corrosion resistance, will be essential for translating intrinsic stability into macroscopic device longevity. Continued reliance on operando spectroscopic tools to monitor degradation mechanisms in real-time under practical operating conditions will remain indispensable. Ultimately, mastering the electronic and structural interplay at coupled active sites will pave the way for the deployment of durable, cost-effective platinum group metal-free energy conversion systems.

References

1. 1. Song, S., Huang, D., Deng, D., Xiong, H., Tang, Y., Zhao, Y., & Qin, R. (2026). Olbedo: An Albedo and Shading Aerial Dataset for Large-Scale Outdoor Environments. In Proceedings of the IEEE/CVF Conference on Computer Vision and Pattern Recognition (pp. 6474-6483).
2. 2. Tian, F., Gao, X., Wu, C., Zhang, L., Xia, X., & Wang, X. (2017). Initial energy supplementation in critically ill patients receiving enteral nutrition: a systematic review and meta-analysis of randomized controlled trials. Asia Pacific Journal of Clinical Nutrition, 26(1), 11-19.
3. 3. Yang, Z., Hu, D., Guo, Q., Zuo, L., & Ji, W. (2023). Visual E 2 C: AI-driven visual end-edge-cloud architecture for 6G in low-carbon smart cities. IEEE Wireless Communications, 30(3), 204-210.
4. 4. Lin, Y., Yao, Y., Zhu, J., & He, C. (2025, July). Application of generative AI in predictive analysis of urban energy distribution and traffic congestion in smart cities. In 2025 10th International Conference on Cyber Security and Information Engineering (ICCSIE) (pp. 620-623). IEEE.

5. 5. Peng, Y., Li, H., BouDagher-Fadel, M., Wang, L., Zhang, D., Zheng, T., & Yang, K. (2022). Benthic foraminifera distribution and sedimentary environmental evolution of a carbonate platform: A case study of the Guadalupian (middle Permian) in eastern Sichuan Basin. Marine Micropaleontology, 170, 102079.
6. 6. Peng, Y., & Li, H. (2023). Benthic foraminiferal morphogroups at the end-Guadalupian extinction in eastern Sichuan Basin, China. Palaeogeography, Palaeoclimatology, Palaeoecology, 618, 111522.
7. 7. Li, H., Zheng, T., Peng, Y., & BouDagher-Fadel, M. K. (2023). The fusulinids in a middle-late Permian carbonate platform (from Maokou to Wuchiapingian stage) in eastern Sichuan Basin, China. In Stratigraphy & Timescales (Vol. 8, pp. 413-435). Academic Press.
8. 8. Yin, L., Ghosh, R., Lin, C., Hale, D., Weigl, C., Obarowski, J., ... & Jin, Z. (2023). Mapping smallholder cashew plantations to inform sustainable tree crop expansion in Benin. Remote Sensing of Environment, 295, 113695.
9. 9. Wang, Y., Lou, M., Luo, Y., Wan, Z., Wang, L., & Tang, Q. (2026). Contact dynamics characteristics of a deepwater drilling riser-drillstring coupled system. Ocean Engineering, 366, 127458.
10. 10. Meng, L., Zhang, B., & Cao, L. (2026). Establishing linear cultural heritage corridors by integrating cultural and ecological values: a case study of the Jinzhong section of the Great Tea Road. Land, 15(2), 293.
11. 11. Liu, Z., Ye, Z., & Zhang, K. (2025). Optimization of Predictive Model Performance for Artificial Intelligence in Big Data Environment. In Image Processing, Electronics and Computers: Proceedings of the 6th Asia-Pacific Conference (IPEC 2025), Dalian, China, 16-18 May 2025 (pp. 1870-1878). 1 Oliver's Yard, 55 City Road, London, EC1Y 1SP: SAGE Publications.
12. 12. Wang, H., Wei, W., Wang, K., Kong, H., Vieira, C. L. Z., Koutrakis, P.,... & Giorio, C. (2025). A global multidimensional analysis of air pollution in land, sea, and air transport cabins reveals substantial health risks. One Earth, 8 (1).
13. 13. Tian, Y. (2026, January). A Data-Driven Energy Efficiency Improvement and Cost Optimisation Model for New Energy Electric Vehicles. In 2026 IEEE International Conference on Power, Electronics and Green Energy (ICPEGE) (pp. 304-308). IEEE.
14. 14. Fan, Y., Hu, C., Wang, Z., Wang, H., Zhang, R., Jiang, D., ... & Koutrakis, P. (2025). Residential VOC from building materials: Exposures, health risks, and ambient hazards.Sustainable Cities and Society,119, 106080.
15. 15. Justice, C. O., Townshend, J. R. G., Vermote, E. F., Masuoka, E., Wolfe, R. E., Saleous, N., Roy, D. P., & Morisette, J. T. (2002). An overview of MODIS land data processing and product status. Remote Sensing of Environment, 83(1–2), 3–15.
16. 16. Gorelick, N., Hancher, M., Dixon, M., Ilyushchenko, S., Thau, D., & Moore, R. (2017). Google Earth Engine: Planetary-scale geospatial analysis for everyone. Remote Sensing of Environment, 202, 18–27.
17. 17. Farr, T. G., Rosen, P. A., Caro, E., Crippen, R., Duren, R., Hensley, S., et al. (2007). The shuttle radar topography mission. Reviews of Geophysics, 45(2), RG2004.
18. 18. Li, Q., Ye, Q., Zhang, N., Zhang, W., & Hu, F. (2025). Digital-twin-enabled industrial IoT: Vision, framework, and future directions. IEEE Wireless Communications, 32(6), 173-181.
19. 19. Pei, Z., Huang, Q., & Wang, S. (2026). When LLMs develop languages: Symbolic communication for efficient multi-agent reasoning. arXiv preprint arXiv:2606.29354.
20. 20. Yang, Z., Ji, W., Guo, Q., & Wang, Z. (2023, October). Javp: Joint-aware video processing with edge-cloud collaboration for dnn inference. In Proceedings of the 31st ACM International Conference on Multimedia (pp. 9152-9160).
21. 21. Prescribed-time tracking control of MIMO nonlinear systems with nonvanishing uncertainties
22. 22. Zou, R., Zhang, Y., Zhao, M., Tan, Z., Zhang, Y., & Cheung, Y. M. (2025). SDENK: Unbiased Subspace Density--Clustering. Neurocomputing, 131225.